

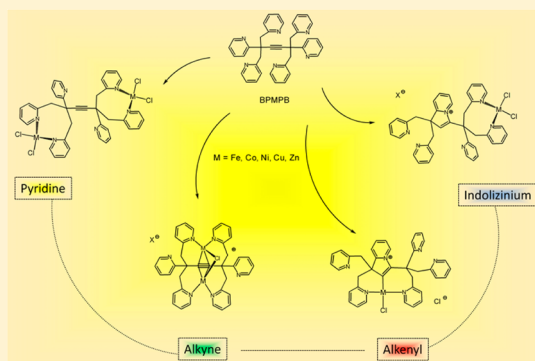
# Versatile Coordination Mode of a New Pyridine-Based Ditopic Ligand with Transition Metals: From Regular Pyridine to Alkyne and Alkenyl Bindings and Indolizinium Formation

Sushil Kumar and Dominique Mandon\*

Laboratoire de Chimie, Electrochimie Moléculaires et Chimie Analytique, UMR 6521, CNRS–Université de Bretagne Occidentale, 6 Avenue Victor Le Gorgeu CS 93837, F-29238 Brest cedex 3, France

## S Supporting Information

**ABSTRACT:** The new BPMPB ligand, namely, bis[1-bis(2-pyridylmethyl),1 (pyridyl)]butyne, can be very easily obtained as a side product in the known reaction of picolyl chloride and sodium acetylide (which major product is the known terminal alkyne-substituted tripod). This symmetrical ligand contains two identical coordination sites with two methylenepyridines and one pyridyl group on each side, linked by an alkyne function providing a semirigid segment. Together with the molecular structure of the ligand which is reported, we describe the preparation of complexes with Fe(II)Cl<sub>2</sub>, Co(II)Cl<sub>2</sub>, Ni(II)Cl<sub>2</sub>, Cu(I)Cl, and Zn(II)Cl<sub>2</sub> salts. All complexes have been characterized by X-ray diffraction studies as well as by standard spectroscopic techniques. The striking point in this work is the diversity of the structures that are obtained. Co(II) and Zn(II) provide isostructural dinuclear complexes in which both coordination sites are occupied within a tetrahedral symmetry. The Cu(I) complex is also a dinuclear compound, but in that case, the copper atom is coordinated to the alkyne moiety, two pyridines, and a bridging chloride. The <sup>13</sup>C NMR spectrum of the copper complex confirms that the metal center is coordinated to the alkyne in solution. The coordination of Ni(II) results in the formation of a mononuclear complex in which a pyridine has fused with the alkyne moiety to generate an indolizinium group; the structure of the corresponding alkenyl complex is reported. Finally, the addition of FeCl<sub>2</sub> to the ligand results in the formation of a mononuclear complex with a free, noncoordinated indolizinium. The sequence developed in the present work illustrates the possibility for the metal centers to adopt various coordination modes which may be relevant to the conversion of an alkyne and a pyridyl unit into indolizinium.



## INTRODUCTION

Tripodal tetraamines with pyridine-containing arms constitute a well-known family of ligands. Both  $\sigma$ -donating tertiary amine and  $\pi$ -accepting pyridyl groups make these ligands excellent chelators that typically coordinate to metal centers in a tetradentate, or tridentate, fashion. With the emblematic representative of this class of compounds, namely the TPA ligand (tris(2-pyridylmethyl)amine), the variety of metal centers range from transition metal complexes to lanthanides and actinides, with applications in various area such as biomimetic chemistry, or material chemistry for instance.<sup>1,2</sup>

Chemical modification of existing ligands is an interesting area, since it can afford compounds with new and sometimes unexpected properties. Within the family of pyridyl-containing ligands, modified compounds providing various coordination modes, or ligand field modulation, for instance, are still under current investigation.<sup>3</sup> These include the family of bispidine,<sup>4–7</sup> N3-Py-R or N4-Py ligands, or hexapyridine dinucleating ligands,<sup>8–13</sup> for example. Considering capping ligands, we were interested in studying simple tripodal ligands in which the amine nitrogen of the tetraamine tripod would be replaced by a carbon atom as is the case for some tripyridine ligands,<sup>13</sup> having

a high flexibility at the coordination site. In these systems, a pure pyridine-based tripod would be linked through the central carbon atom to a fourth arm, with this latter being potentially functionalized, and able to subsequently react with various substrates, or reactive groups. The alkyne-substituted tripod **A** in Figure 1, namely, the bis(2-pyridylmethyl)(pyridyl)propyne, would be supposed to fulfill these requirements. Indeed, its synthesis was reported together with the formation of compound **B**, the tris(2-pyridylmethyl)pyridylmethane tetrapod, obtained as a minor component.<sup>14,15</sup>

Ligand **A** was prepared according to the procedure reported in 1974.<sup>14</sup> We got this compound as the main product of the reaction together with the new symmetrical ditopic ligand **L** = BPMPB drawn in Figure 1, and some 1,2-*trans*-bis(2-pyridyl)-ethylene. We thus decided to investigate the reactivity of BPMPB. This new ligand, being very easy to obtain, turned out to be very stable and reacted with various metal salts of the first series to provide several new compounds. In particular, those included complexes in which part of the ligand was converted

Received: May 15, 2015

Published: July 22, 2015

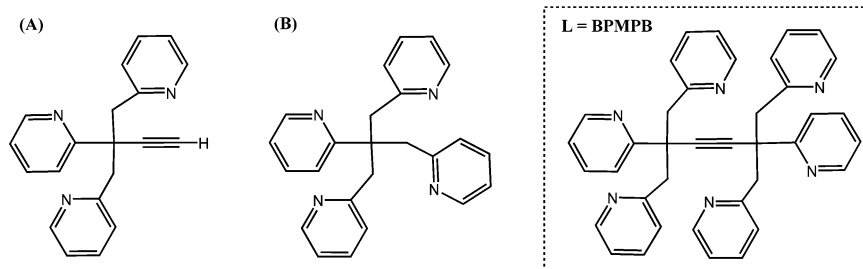


**Figure 1.** Bis(2-pyridylmethyl)(pyridyl)propyne (A) and tris(2-pyridylmethyl)pyridylmethane (B) compounds as reported in the literature,<sup>14</sup> together with the new bis[1-bis(2-pyridylmethyl),1 (pyridyl)]butyne ligand (BPMPB) reported in the present study (right, in frame).

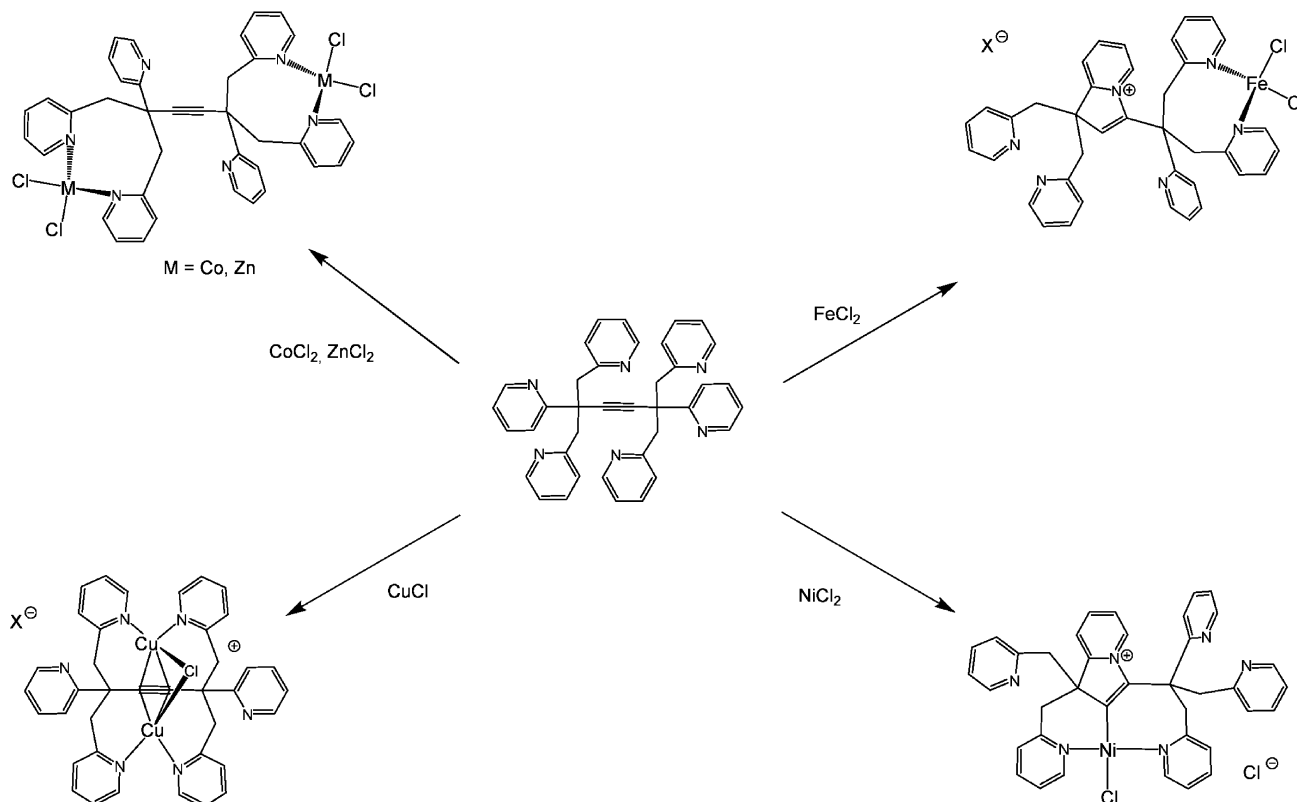


**Figure 2.** Versatile coordination chemistry of the BPMPB ligand reported in this Article.

to an indolizinium cation, the formation of which involves fusion of the alkyne part of the ligand with one pyridine, which in the present case is metal-dependent.

In the present contribution, we wish to disclose our results on the coordination chemistry of the BPMPB ligand with Fe, Co, Ni, Cu, and Zn salts (Figure 2). Following the description of the structure of this new ligand, XRD studies of several complexes are reported. These include mononuclear or dinuclear compounds containing bridging-alkyne, alkenyl ligand resulting from fused alkyne/pyridyl units, or the free indolizinium ring. In the last case, the indolizinium could represent the ultimate step in the conversion of an alkyne and pyridyl unit into such an heterocycle.<sup>16</sup>

## EXPERIMENTAL SECTION

**General Considerations.** Chemicals were purchased from Aldrich Chemicals and used as received. Unless otherwise stated, all the solvents used during the metalation reactions and workup were distilled and dried according to standard methods [Armarego, W. L. F., Perrin, D. D. *Purification of Laboratory Chemicals*, 4th ed.; Pergamon

Press: Oxford, 1997]. Alternatively, they could be obtained from a solvent purification device (MBRAUN). Preparation and handling of all the compounds were performed under an argon atmosphere by using the Schlenk technique following standard procedures. Mass spectrometric experiments were carried out by the “Service Commun de Spectrométrie de Masse de l’UBO”, Brest. All XRD experiments were carried out by the “Service Commun de Diffraction X de la Faculté des Sciences et Techniques de l’UBO”, Brest. The elemental analyses were carried out by the “Service de Microanalyses de l’ICSN, Gif sur Yvette”, and the “Service Central d’Analyses de l’ISA, Lyon”.

**Physical Methods.** The  $^1\text{H}$  NMR data were recorded in  $\text{CDCl}_3$ ,  $\text{CD}_2\text{Cl}_2$  or  $(\text{CD}_3)_2\text{SO}$  for the ligand as well as metal complexes at ambient temperature on a Bruker AC 300 spectrometer at 300.1300 MHz with the residual signal of  $\text{CHCl}_3$ ,  $\text{CDHCl}_2$  and  $[(\text{CD}_3\text{H})_2\text{SO}]$  as a reference for calibration. The IR spectra were recorded on a Bruker Vertex 70 spectrometer. The UV–vis spectra were recorded on a Varian Cary 05 E UV–vis–NIR spectrophotometer equipped with an Oxford instrument DN1704 cryostat with optically transparent Schlenk cells.

The effective magnetic moments ( $\mu_{\text{eff}}$ 's) for paramagnetic species were determined in solution by  $^1\text{H}$  NMR (Avance 400 BRUKER, or DRX 300 BRUKER) at room temperature using the Evans

method,<sup>17,18</sup> with tetramethylsilane (TMS) as an internal standard. Diamagnetic corrections have been applied using Pascal constants.<sup>19</sup>

**Reaction of Picolyl Chloride with Sodium Acetylide, and Synthesis of the Bis[1-bis(2-pyridylmethyl),1 (pyridyl)]butyne Ligand (BPMPB).** A slurry of 24 mmol of sodium acetylide (6.4 g of suspension in xylene/mineral oil, 18 wt %) was introduced in a well-dried Schlenk tube. An ammonia gas cylinder was fitted to the Schlenk tube, and about 50 mL of liquid NH<sub>3</sub> was condensed maintaining the temperature around -70 °C. After removal of the cylinder, 3.0 g of 2-chloromethylpyridine (24 mmol) was added dropwise to ammoniacal solution in the course of 5 min which resulted in the formation of a white precipitate. The reaction mixture was stirred for 3–4 h while the liquid ammonia was evaporated slowly. The resulting dark brown pasty residue was quenched with ice-cold water and was filtered using a suction pump. The light brown precipitate was washed 2–3 times with pentane and diethyl ether and was recrystallized from dichloromethane/hexane mixture to get white crystals of compound BPMPB with an 18.5% yield.

<sup>1</sup>H NMR, 298 K, CDCl<sub>3</sub>,  $\delta$ , ppm: 8.66 (d, 2H), 8.32 (d, 4H), 7.27–6.93 (m, 14H), 6.56 (d, 4H), 3.60 (AB system, -CH<sub>2</sub>- protons, <sup>HHJ</sup> = 12.7 Hz).

<sup>13</sup>C NMR, 298 K, CDCl<sub>3</sub>,  $\delta$ , ppm: 48.68, 48.78, 89.40, 120.65, 120.93, 122.77, 124.35, 134.68, 135.16, 148.00, 148.28, 157.91, and 160.57.

UV-vis, 298 K, CH<sub>2</sub>Cl<sub>2</sub>,  $\lambda_{\max}/\text{nm}$ ,  $\epsilon$ , M<sup>-1</sup> cm<sup>-1</sup>: 262 (20 800).

IR: 1587, 1566, 1467, 1431, 1339, 1088, 1050, 994, 785, 770, 745, and 578 cm<sup>-1</sup>.

MS, ESI, positive,  $m/z$  = 573, [M + H]<sup>+</sup>; 595, [M + Na]<sup>+</sup>.

Anal. Calcd C<sub>38</sub>H<sub>32</sub>N<sub>6</sub>, %: C, 79.7; H, 5.6; N, 14.7. Found: C, 79.4; H, 5.7; N, 14.4.

The filtrate was extracted with diethyl ether, dried over sodium sulfate, and concentrated under vacuum. The dark crude material was placed on an alumina column. A very light yellow compound was eluted as the first fraction with diethyl ether. White single crystals of *trans*-1,2-dipyridyl ethene were obtained by slow evaporation of the solution of compound in dichloromethane/diethyl ether mixture. Yield 20.8%.

<sup>1</sup>H NMR, 298 K, CDCl<sub>3</sub>,  $\delta$ , ppm: 8.60–7.10 ppm (10H, all expected aromatic and alkene protons).

<sup>13</sup>C NMR, 298 K, CDCl<sub>3</sub>,  $\delta$ , ppm: 122.16, 122.86, 131.24, 136.17, and 149.29.

MS, ESI, positive,  $m/z$  = 183, [M + H]<sup>+</sup>.

A yellow liquid was eluted as the second component from a column with a diethyl ether/acetone (1:1) mixture, to yield an oily compound which was identified as compound A of Figure 1 and characterized by comparison of its <sup>1</sup>H and <sup>13</sup>C NMR spectra with those already published. Yield 41.7%.

<sup>1</sup>H NMR, 298 K, CD<sub>2</sub>Cl<sub>2</sub>,  $\delta$ , ppm: 8.66 (d, 1H), 8.38 (d, 2H), 7.52–6.90 (m, 9H), 3.71 (AB system, -CH<sub>2</sub>-, 2H), 3.46 (AB system, -CH<sub>2</sub>-, 2H) and 2.51 (s, 1H) ppm. <sup>13</sup>C NMR, 298 K, CD<sub>2</sub>Cl<sub>2</sub>,  $\delta$ , ppm: 49.02, 49.30, 76.71, 85.89, 121.60, 122.04, 123.00, 124.95, 135.47, 136.22, 148.92, 149.15, 158.36, and 160.96 ppm.

**Preparation of the BPMPBM<sub>2</sub>Cl<sub>4</sub> Complexes.** All the complexes were prepared by following a general procedure. Details are given for (BPMPB)Zn<sub>2</sub>Cl<sub>4</sub>, but the following procedure applies for all complexes. The reactions were carried out under inert atmosphere in all the cases except complex (BPMPB)Zn<sub>2</sub>Cl<sub>4</sub>.

**[(BPMPB)Zn<sub>2</sub>Cl<sub>4</sub>].** A batch of 0.029 g (0.05 mmol) of ligand (BPMPB) was dissolved in 20 mL of distilled dichloromethane to obtain a colorless solution. A 0.014 g portion of anhydrous ZnCl<sub>2</sub> (0.1 mmol) was introduced to the reaction vessel, and the mixture was stirred at room temperature for 5–6 h. A white suspension was obtained. The medium was concentrated to 10 mL under vacuum, and 20–30 mL of diethyl ether was added to obtain the desired compound as white precipitate (0.025 g, 0.029 mmol, 58% yield), which was dried under vacuum.

Single crystals of complex for X-ray diffraction were grown by slow diffusion of diethyl ether into a solution of compound in dichloromethane/methanol mixture at room temperature.

<sup>1</sup>H NMR, 298 K, CD<sub>2</sub>Cl<sub>2</sub>,  $\delta$ , ppm: 9.08, 1H,  $\alpha$ -py; 9.03, 2H,  $\alpha$ -py; 8.87, 1H,  $\alpha$ -py; 8.27, 2H,  $\alpha$ -py; 7.94–7.23, m, 15H, aromatics; 6.70, 1H, aromatics; 6.20, 2H, aromatics; 4 AB systems corresponding to the methylene protons,  $\delta$  = 3.50 ppm (<sup>HHJ</sup> = 14.2 Hz),  $\delta$  = 3.44 ppm (<sup>HHJ</sup> = 13.8 Hz),  $\delta$  = 3.37 ppm (<sup>HHJ</sup> = 14.1 Hz), and  $\delta$  = 3.36 ppm (<sup>HHJ</sup> = 13.9 Hz).

DMSO-*d*<sub>6</sub>,  $\delta$ , ppm: 8.58, 3H,  $\alpha$ -py; 8.35, 1H,  $\alpha$ -py; 8.30, 2H,  $\alpha$ -py; 8.11, 1H, aromatics; 7.80–6.92, aromatics + broad signals at 298 K; 2 AB systems corresponding to the methylene protons,  $\delta$  = 3.55 ppm (<sup>HHJ</sup> = 12.7 Hz) and  $\delta$  = 3.43 ppm (<sup>HHJ</sup> = 13.1 Hz).

Variable temperature spectra displayed in the [Supporting Information](#).

IR: 1607, 1571, 1487, 1469, 1440, 1325, 1160, 1027, 774, 577, and 424 cm<sup>-1</sup>.

UV-vis, 298 K, CHCl<sub>3</sub>,  $\lambda_{\max}/\text{nm}$ ,  $\epsilon$ , M<sup>-1</sup> cm<sup>-1</sup>: 264 (13 378), 272 (9622).

DMSO,  $\lambda_{\max}/\text{nm}$ ,  $\epsilon$ , M<sup>-1</sup> cm<sup>-1</sup>: 263 (11 000), 270 (8293).

MS, ESI, positive,  $m/z$  = 671.1737; [BPMPBZnCl]<sup>+</sup> and 573.2822; [BPMPBH]<sup>+</sup>.

Anal. Calcd C<sub>38</sub>H<sub>32</sub>Zn<sub>2</sub>Cl<sub>4</sub>N<sub>6</sub>·CH<sub>2</sub>Cl<sub>2</sub>, %: C, 50.5; H, 3.7; N, 9.0; Found: C, 50.9; H, 3.9; N, 8.8.

**[(BPMPB)Co<sub>2</sub>Cl<sub>4</sub>].** Blue, yield 72%. To obtain the single crystals of the complex for X-ray diffraction, a dichloromethane solution of complex was layered with hexane for 2 days at room temperature.

<sup>1</sup>H NMR, 298 K, CDCl<sub>3</sub>,  $\delta$ , ppm ( $\Delta_{\nu/2}$ , Hz): 62 (73), 61 (98), 57 (55), 56 (55), 43 (73), 41 (73), 40 (83), 39 (114), 36 (65), 17 (140), 14 (100), 13 (115), 11 (100), + sharper signals between 8 and 0 ppm. Spectrum displayed in the [Supporting Information](#).

IR: 1655, 1605, 1569, 1484, 1433, 1296, 1102, 1027, 772, and 576 cm<sup>-1</sup>.

UV-vis, 298 K, CHCl<sub>3</sub>,  $\lambda_{\max}/\text{nm}$ ,  $\epsilon$ , M<sup>-1</sup> cm<sup>-1</sup>: 264 (8885), 574 (423), 611 (615), 633 (615).

MS, ESI, positive,  $m/z$  = 702.1448; [BPMPBHCoCl<sub>2</sub>]<sup>+</sup>, 666.1689; [BPMPBCoCl]<sup>+</sup> and 573.2750; [BPMPBH]<sup>+</sup>;  $m/z$  = 315.6020; [BPMPBCo]<sup>2+</sup>.

Anal. Calcd C<sub>38</sub>H<sub>32</sub>Co<sub>2</sub>Cl<sub>4</sub>N<sub>6</sub>·1/2CH<sub>2</sub>Cl<sub>2</sub>, %: C, 52.9; H, 3.8; N, 9.6; Found: C, 53.0; H, 3.9; N, 9.2.

Magnetic susceptibility (DRX 300 BRUKER):  $\mu_{\text{eff}}$  = 6.06  $\mu\text{B}$  (CD<sub>2</sub>Cl<sub>2</sub>, Evans method).  $\Delta\nu$  = 39.61 Hz, for a 2 mM solution. Diamagnetic correction: -0.000 391 emu/mol.

**[(BPMPB)Cu<sub>2</sub>Cl]<sub>2</sub>Cl.** Colorless, yield 66% from 3 equiv of CuCl per ligand. In this case, the complex [(BPMPB)Cu<sub>2</sub>Cl]CuCl<sub>2</sub> is obtained, and it displays the same spectroscopic data. To obtain single crystals of the complex for X-ray diffraction, diethyl ether was diffused slowly into a dichloromethane solution of complex at room temperature.

<sup>1</sup>H NMR, 298 K, CDCl<sub>3</sub>,  $\delta$ , ppm: 8.57, 6H,  $\alpha$ -py; 7.80–7.08, 18H, aromatics; 1 AB system, 8H, centered at  $\delta$  = 3.72 ppm (<sup>HHJ</sup> = 13.9 Hz). Spectrum displayed in the [Supporting Information](#).

IR: 1601, 1567, 1476, 1439, 1259, 1055, 791, 701, 661, and 452 cm<sup>-1</sup>.

UV-vis, 298 K, CH<sub>2</sub>Cl<sub>2</sub>,  $\lambda_{\max}/\text{nm}$ ,  $\epsilon$ , M<sup>-1</sup> cm<sup>-1</sup>: 263 (20 583), 308 (sh, 5458).

Anal. Calcd C<sub>38</sub>H<sub>32</sub>Cu<sub>2</sub>Cl<sub>3</sub>N<sub>6</sub>·1/2CH<sub>2</sub>Cl<sub>2</sub>, %: C, 50.7; H, 3.6; N, 9.2. Found: C, 50.9; H, 3.8; N, 8.7.

**[(InBPMPB)NiCl]<sub>2</sub>Cl.** Green, yield 66%. To obtain the single crystals of the complex for X-ray diffraction, diethyl ether was allowed to slowly diffuse into a solution of complex in a dichloromethane/methanol mixture.

<sup>1</sup>H NMR, 298 K, CDCl<sub>3</sub>,  $\delta$ , ppm ( $\Delta_{\nu/2}$ , Hz): 212 (900), 184 (900), 62 (315), 57 (310), 45 (310), 39 (320), 26 (305), 23 (300), -5 (290), -8 (315) + sharper signals between 11 and 3 ppm. Spectrum available in the [Supporting Information](#).

IR: 1623, 1605, 1589, 1568, 1476, 1434, 1261, 1102, 995, 759, 581, and 462 cm<sup>-1</sup>.

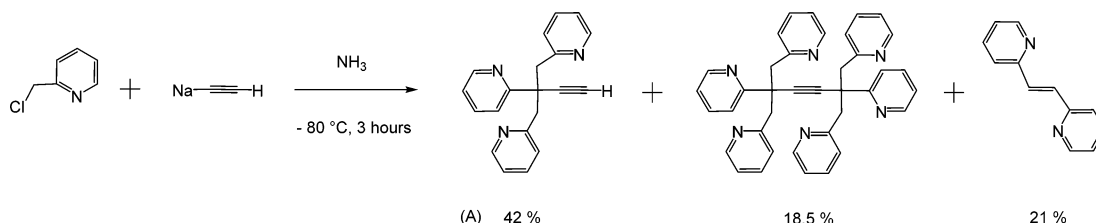
UV-vis, 298 K, CH<sub>2</sub>Cl<sub>2</sub>,  $\lambda_{\max}/\text{nm}$ ,  $\epsilon$ , M<sup>-1</sup> cm<sup>-1</sup>: 264 (27 042), 371 (4667).

MS, ESI, positive,  $m/z$  = 665.1680; [InBPMPBNi-Cl]<sup>+</sup>, 573.2728; [InBPMPB]<sup>+</sup>;  $m/z$  = 315.1014; [InBPMPBNi]<sup>2+</sup>.

Anal. Calcd C<sub>38</sub>H<sub>32</sub>NiCl<sub>2</sub>N<sub>6</sub>·CH<sub>2</sub>Cl<sub>2</sub>, %: C, 59.5; H, 4.3; N, 10.7. Found: C, 59.2; H, 4.6; N, 10.4.



Scheme 1. Access to the BPMPB Ligand by Reaction of Picolyl Chloride with Sodium Acetylide



Magnetic susceptibility (Avance 400 BRUKER):  $\mu_{\text{eff}} = 2.89 \mu\text{B}$  ( $\text{CD}_2\text{Cl}_2$ , Evans method).  $\Delta\nu = 5.22 \text{ Hz}$ , for a 1.6 mM solution. Diamagnetic correction:  $-0.000335 \text{ emu/mol}$ .

$[(\text{HInBPMPB})\text{FeCl}_2][\text{Cl}]$ . Light brown, yield 60%. To obtain the single crystals of complex  $[(\text{HInBPMPB})\text{FeCl}_2][\text{FeCl}_4]$  for X-ray diffraction, a solution of complex in dichloromethane/methanol mixture was layered with hexane for 2–3 days under inert atmosphere.

$^1\text{H}$  NMR, 298 K,  $\text{CDCl}_3$ ,  $\delta$ , ppm ( $\Delta_{\nu/2}$ , Hz): 77 (720), 46 (390), + a series of broad signals at  $\delta = 13$  (26), 10 (47), 8 (52), 6 (70), 5 (58), 4 (43), 3 (29) ppm. Spectrum available in the [Supporting Information](#).

IR: 1626, 1588, 1473, 1434, 1261, 1151, 1097, 1052, 994, 857, 780, 751, 567, and  $467 \text{ cm}^{-1}$ .

UV–vis, 298 K,  $\text{CH}_2\text{Cl}_2$ ,  $\lambda_{\text{max}}/\text{nm}$ ,  $\epsilon$ ,  $\text{M}^{-1} \text{ cm}^{-1}$ : 261 (23 250), 296 (sh, 11 250), 364 (4450).

MS, ESI, positive,  $m/z = 573.2828$ ;  $[\text{BPMPBH}]^+$ .

Anal. Calcd  $\text{C}_{38}\text{H}_{33}\text{FeCl}_3\text{N}_6 \cdot 2\text{CH}_2\text{Cl}_2$ , %: C, 53.0; H, 3.9; N, 9.7. Found: C, 53.0; H, 4.1; N, 9.3.

Magnetic susceptibility (DRX 300 BRUKER) on single crystals dissolved in  $\text{CD}_2\text{Cl}_2$ :  $\mu_{\text{eff}} = 8.71 \mu\text{B}$  ( $\text{CD}_2\text{Cl}_2$ , Evans Method).  $\Delta\nu = 47.31 \text{ Hz}$ , for a 1.2 mM solution. Diamagnetic correction:  $-0.000726 \text{ emu/mol}$ .

**X-ray Analysis.** The single crystals were mounted on a Xcalibur-2 diffractometer from Oxford Diffraction (Mo  $K\alpha$ ,  $\lambda = 0.71073 \text{ \AA}$ ). Quantitative data were obtained at 170 K for all the compounds. The crystal data collection and processing were performed with CRYSTALIS software (CrysAlis CCD and CrysAlis RED; Oxford Diffraction Ltd.: Abingdon, Oxford, United Kingdom, 2009). The cell parameters were determined using all the frames. All structures were solved using SIR92<sup>20</sup> and SHELXS-97 (Sheldrick, G. M. SHELXS-97: Program for Crystal Structure Solution; University of Göttingen: Göttingen, Germany, 1997), and were refined by full-matrix least-squares on  $F^2$  using the SHELXL-97. The absorption was corrected empirically and analytically. All non-hydrogen atoms were refined anisotropically. Hydrogen atoms were generated according to stereochemistry and refined using a riding model in SHELXL97. Molecular graphics were created with the DIAMOND program (Brandenburg, K. DIAMOND: Program for Crystal and Molecular Structure Visualization; Crystal Impact GbR: Bonn, Germany, 2011).

## RESULTS

**BPMPB Ligand: Preparation and Structure.** The early report of the preparation of the (2-pyridylmethyl)(pyridyl)propyne ligand (A in [Figure 1](#)) involved the reaction of equimolar amounts of 2-chloromethylpyridine and sodium acetylide generated in situ in liquid ammonia.<sup>14</sup> Small amounts of the tris(2-pyridylmethyl)pyridylmethane tetrapod (B of [Figure 1](#)) were also obtained. The yield of A + B was reported as being quantitative. The ligands were characterized by the available techniques such as melting point, infrared spectroscopy, elemental analysis, and  $^1\text{H}$  and  $^{13}\text{C}$  NMR spectroscopy with the resolution available at this time (1974). We reproduced the published procedure, with the only modification being that we used sodium acetylide from a commercial source, provided as a slurry in a mixture of mineral oil and xylenes. The reaction was carried out in a Schlenk tube under controlled atmosphere, in liquid ammonia. The result of this

reaction is outlined in [Scheme 1](#). At the first step of the workup, a white solid could easily be separated from an oily residue, as mentioned in the original paper.

The oily liquid was treated and turned out to contain some ligand A that was recovered by chromatographic treatment, with a yield of 42% with respect to the pyridine. This compound, already known, was first characterized by ESI MS, and then by  $^1\text{H}$  NMR and  $^{13}\text{C}$  NMR spectroscopy with the data matching those already reported.<sup>14,15</sup> In the course of the workup, the known (and commercially available) 1,2-bis(2-pyridyl)ethyne compound was also isolated as a white solid in 21% yield,<sup>21</sup> and characterized by  $^1\text{H}$  and  $^{13}\text{C}$  NMR, and eventually by XRD (the crystal structure was already published and will not be shown here).<sup>22</sup> Finally, it should be mentioned here that, in our hands, tetrapod B, drawn in [Figure 1](#) and mentioned as a minor product in the original paper, could not be obtained.

The white solid which separated from the oily residue is particularly easy to obtain. It turned out to be the BPMPB ligand, obtained as the minor product of this reaction since the yield is 18.5%. It was characterized by mass spectroscopy with an  $m/z$  signal at 573.269 for  $\text{BPMPBH}^+$ , and by  $^1\text{H}$  and  $^{13}\text{C}$  NMR spectroscopy. In principle, BPMPB is a symmetrical molecule: this is evidenced by the observation of identical aromatic resonances for all pyridylmethyl, and pyridyl, protons, respectively. The methylene groups, however, are magnetically nonequivalent, and appear as an AB system, centered at  $\delta = 3.60 \text{ ppm}$  ( $J_{\text{HH}} = 12.7 \text{ Hz}$ ). The  $^{13}\text{C}$  spectrum does not lead to any particular comment, with the alkyne carbon appearing at  $\delta = 89.4 \text{ ppm}$ . The UV–vis spectrum of the free BPMPB ligand in methylene chloride consisted of a single absorption at  $\lambda = 262 \text{ nm}$  ( $\epsilon = 20\,800 \text{ L mol}^{-1} \text{ cm}^{-1}$ ). All traces are given in the [Supporting Information](#).

Single crystals of the BPMPB ligand could be obtained by slow evaporation of a solution of the compound in dichloromethane/hexane mixture, and the structure was solved by X-ray analysis. The ORTEP diagram is displayed in [Figure 3](#).

As expected, a short distance  $d\text{C1}–\text{C}'1 = 1.191(2) \text{ \AA}$  is found for the triple bond. The distance  $d\text{C1}–\text{C}2 = 1.472(2) \text{ \AA}$  is relatively short and indicates some degree of delocalization of the triple bond between these atoms. This makes the heart of the ligand somewhat rigid, with a distance of  $4.134(2) \text{ \AA}$  between both quaternary carbon atoms C2 and C'2. Additionally, short contacts  $d\text{N2}–\text{H9B} = 2.591(2) \text{ \AA}$  and  $d\text{N2}–\text{H3B} = 2.538(2) \text{ \AA}$  indicate hydrogen bonding between the pyridine and the adjacent methylene groups, which assign the conformation to this ligand in the solid state.

**Preparation of the Metal Complexes.** All metal complexes reported in this Article were obtained by reaction of 2 or 3 equiv of  $\text{MCl}_2$  ( $\text{M} = \text{Fe}, \text{Co}, \text{Ni}, \text{Zn}$ ) or  $\text{MCl}$  ( $\text{M} = \text{Cu}$ ) with 1 equiv of BPMPB. The nickel and cobalt salts were in the hexahydrated form  $\text{NiCl}_2 \cdot 6 \text{H}_2\text{O}$  and  $\text{CoCl}_2 \cdot 6 \text{H}_2\text{O}$ . The solvent was methylene chloride, and all preparations were

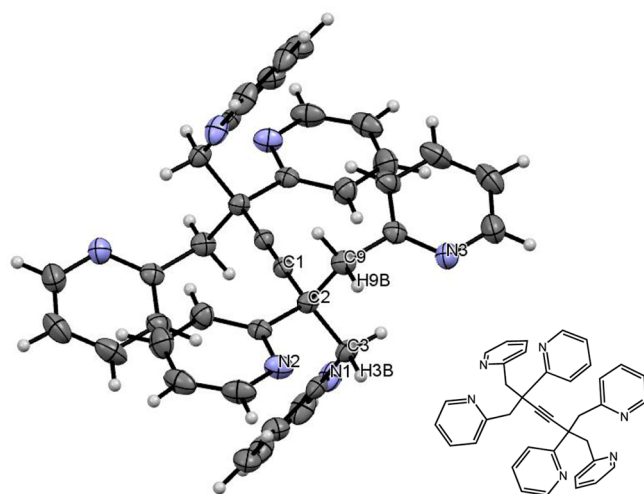


**Figure 3.** ORTEP diagram of the BPMPB ligand, with partial numbering. This compound has an inversion symmetry: bond distances and angles are identical for the inversion counterpart (identical labeling with a ' superscript). Selected distances in Å:  $d_{C1-C'1}$ , 1.191(2);  $d_{C1-C2}$ , 1.472(2);  $d_{C2-C'2}$ , 4.134(2).

carried out under inert atmosphere. After reaction, the mixture was concentrated and the solid complex obtained by precipitation with diethyl ether, a solvent from which they were generally recrystallized. Depending on the preparation, the yields in crystalline material were ca. 60–70%.

**Tetragonal Complexes with Unmodified Ligand: Zinc and Cobalt Complex.** The zinc complex was obtained as a white solid. With a main absorption at  $\lambda = 264$  nm ( $\epsilon = 13\,378$  M<sup>-1</sup> cm<sup>-1</sup>), the UV–vis spectrum does not qualitatively differ from that of the free ligand. In <sup>1</sup>H NMR in CD<sub>2</sub>Cl<sub>2</sub> at room temperature, four AB systems appear in the methylene region, at  $\delta = 3.50$  ppm ( $J_{HH} = 14.2$  Hz),  $\delta = 3.44$  ppm ( $J_{HH} = 13.8$  Hz),  $\delta = 3.37$  ppm ( $J_{HH} = 14.1$  Hz), and  $\delta = 3.36$  ppm ( $J_{HH} = 13.9$  Hz). Obviously, the symmetry is broken in this complex, and this is confirmed by the presence of four distinct signals corresponding to the two distinct  $\alpha$  protons of the pyridines ( $\delta = 9.1$  and  $8.9$  ppm, 1H each) and two pairs of  $\alpha$  protons of the pyridyl groups bound by a methylene bridge ( $\delta = 9.0$  and  $8.3$  ppm, 2H each). Since the signals in the aromatic region

appeared as slightly broadened, measurements were performed at lower temperature, 273, 263, and 243 K. As a result, from 273 to 243 K, the resolution was found to be significantly improved, with no other modification in the position of the signals, suggesting the occurrence of some limited dynamic effect in solution at ambient temperature. Data could also be obtained in DMSO-*d*<sub>6</sub>, solvent which provided a significantly different spectrum, with some broadened signals in the aromatic region, along with well-resolved resonances. In this case, only two AB systems were observed at  $\delta = 3.55$  ppm ( $^{HH}J = 12.7$  Hz) and  $\delta = 3.43$  ppm ( $^{HH}J = 13.1$  Hz). The spectrum was also recorded at 333 K, the temperature at which the broad resonances were replaced by highly resolved signals. DMSO is a polar and highly dissociating solvent. It is likely that the chloride ligands may exchange, at room temperature with the solvent or with water present in the solution. At the time scale of the NMR at room temperature, this exchange would affect some signals in the aromatic region while it would be invisible at higher temperature. To conclude, both UV–vis and NMR studies suggest a solvent-dependent coordination for this complex. The room temperature spectra are displayed in [Figure 4](#). All UV–vis and variable temperature NMR traces are given in the [Supporting Information](#).

The cobalt complex is a blue solid, with absorptions in the UV–vis range at  $\lambda = 264$ , 574, 611, and 633 nm ( $\epsilon = 8885$ , 423, 615, and 615 L mol<sup>-1</sup> cm<sup>-1</sup>, respectively). The <sup>1</sup>H NMR spectrum of this complex exhibited paramagnetically shifted and broadened signals, together with sharper ones in the diamagnetic region. The spectrum, which could not be easily assigned, is displayed in the [Supporting Information](#). Magnetic susceptibility measurements were carried out by the Evans method. The magnetic moment  $\mu_{\text{eff}} = 6.06$   $\mu_B$  was found to be slightly higher than the expected spin-only moment for a two independent center species ( $\mu_{\text{eff}} = 5.48$   $\mu_B$ ).

Single crystals of both compounds could be obtained by diffusion of diethyl ether in a solution of methylene chloride/methanol for the zinc complex, and hexane in a solution of methylene chloride for the cobalt complex. Structural determination was possible for these two compounds. The ORTEP diagrams are displayed in [Figure 5](#).

At first glance both compounds look isostructural: this is true at the molecular level only, and is obvious from the ORTEP

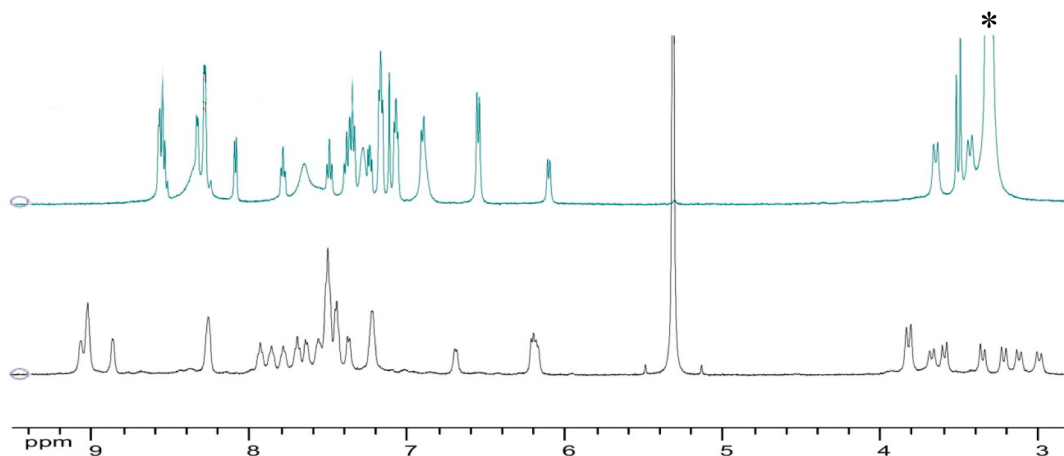


**Figure 4.** Comparison between the room temperature <sup>1</sup>H NMR spectra of BPMPBZn<sub>2</sub>Cl<sub>4</sub> in CD<sub>2</sub>Cl<sub>2</sub> (lower) and DMSO-*d*<sub>6</sub> (upper trace). At this temperature, the CD<sub>2</sub>Cl<sub>2</sub> spectrum exhibits slightly broadened signals in the aromatic region. All variable temperature spectra are shown in the [Supporting Information](#). The asterisk corresponds to the presence of water in DMSO.

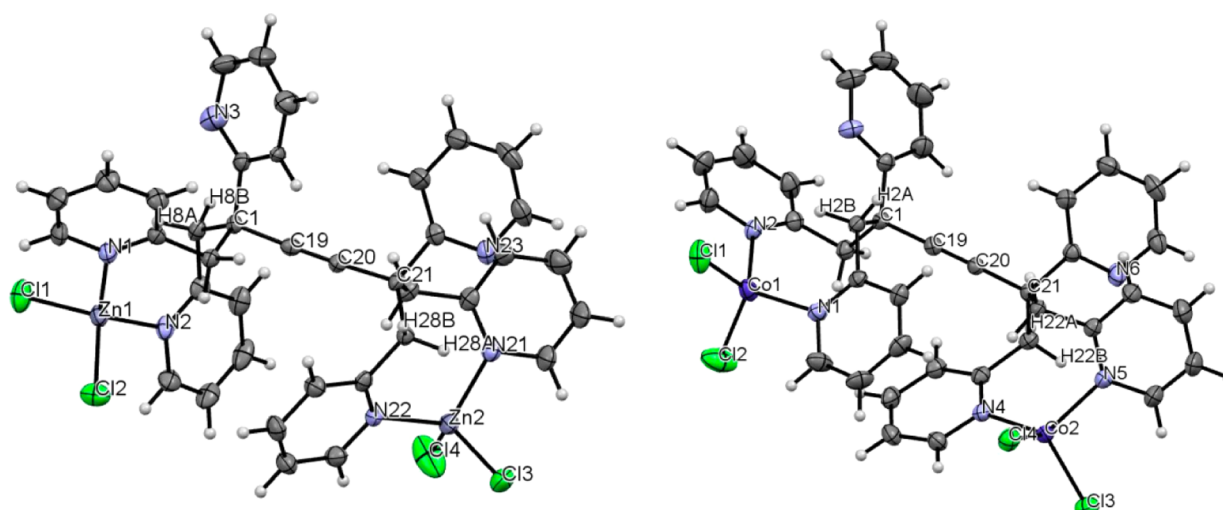


Figure 5. ORTEP diagrams of BPMPBZn<sub>2</sub>Cl<sub>4</sub> (left) and BPMPBCo<sub>2</sub>Cl<sub>4</sub> (right).

Table 1. Metal-to-Ligand Distances in the BPMPBZn<sub>2</sub>Cl<sub>4</sub> and BPMPBCo<sub>2</sub>Cl<sub>4</sub> Complexes

	M1–Cl1	M1–Cl2	M1–N1	M1–N2	M2–Cl3	M2–Cl4	M2–N21/M2–N5	M2–N2/M2–N4
BPMPBZn <sub>2</sub> Cl <sub>4</sub>	2.2252(13)	2.2312(13)	2.042(4)	2.049(3)	2.2365(14)	2.2174(15)	2.036(4)	2.049(3)
BPMPBCo <sub>2</sub> Cl <sub>4</sub>	2.234(2)	2.225(2)	2.042(6)	2.038(7)	2.224(2)	2.243(2)	2.046(6)	2.046(6)

diagrams which display identical structures. However, they have different symmetry and space groups.

The structure consists of the BPMPB ligand in which the pyridines of the methylenepyridine arms coordinate to the metal dichloride. The pyridyl groups which are directly linked to the carbon skeleton are free, but in interaction with two protons of an adjacent methylene, as this was the case for the free BPMPB ligand. For both complexes, the corresponding contacts lie in the range  $2.56 < d_{\text{N}_{\text{py}}-\text{CH}_2} < 2.76$  Å. The central triple bond is short, with  $d_{\text{C19}-\text{C20}} = 1.191(5)$  and  $1.180(9)$  Å for the zinc and cobalt complex, respectively. The principal metric parameters of both complexes are summarized in Table 1.

**Coordination of the Metal to Methylenepyridines and the Triple Bond: [BPMPBCu<sub>2</sub>Cl]Cl.** The Cu(I) complex was obtained as a white solid, and characterized using different spectroscopic techniques. Its UV–vis spectrum in methylene chloride mainly consists of the ligand centered absorption at  $\lambda = 263$  ( $\epsilon = 20\,583$  L mol<sup>−1</sup> cm<sup>−1</sup>) and a shoulder near 308 nm ( $\epsilon = 5458$  L mol<sup>−1</sup> cm<sup>−1</sup>). The <sup>1</sup>H NMR spectrum of [BPMPBCu<sub>2</sub>Cl]Cl in CD<sub>2</sub>Cl<sub>2</sub> looks simple: the methylene groups appear as a broadened AB system, centered at  $\delta = 3.72$  ppm ( $J_{\text{HH}} = 13.9$  Hz), and the aromatic protons between 7.0 and 8.6 ppm as slightly broadened signals. By contrast with the zinc complex, a symmetry similar to that of the free ligand is observed in this complex. In <sup>13</sup>C NMR, the most striking feature is the important upfield shift of the alkyne carbons which appear at  $\delta = 54.9$  ppm whereas they were observed at  $\delta = 89.4$  ppm in the free ligand. This supports a strong interaction between the metal and the triple bond in solution. Finally, we may mention that, in the former preparations, 2 equiv of Cu(I)Cl were reacted with BPMPB to afford a cationic species with Cl<sup>−</sup> as the counteranion. At this stage, we decided to use 3 equiv of metal salt which allowed us to get easily, by simple precipitation, a microcrystalline material with the CuCl<sub>2</sub><sup>−</sup> anion, having the same spectroscopic properties.

Single crystals of this complex could be obtained by slow diffusion of diethyl ether into a methylene chloride solution, and the structure could be resolved. The first thing to note is that the complex is an ionic compound: the well-known cuprate CuCl<sub>2</sub><sup>−</sup> anion is present in the structure together with the dinuclear BPMPBCu<sub>2</sub>Cl<sup>+</sup> cation. The ORTEP diagram of the cationic complex is displayed in Figure 6.

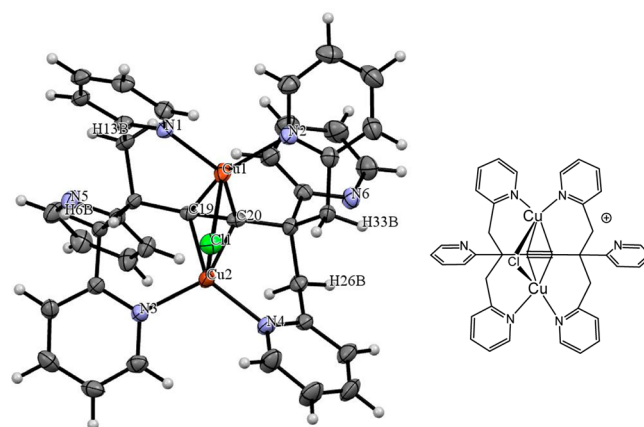


Figure 6. ORTEP diagram of the BPMPBCu<sub>2</sub>Cl<sup>+</sup> complex with partial labeling.

In this complex, each copper atom coordinates to two pyridines from different segments (i.e., from either side of the alkyne bond), to a bridging chlorine atom, and to the triple bond through the carbons C19 and C20. If one approximates that the copper atom is being directly linked to the middle of the triple bond (instead of carbons C19 and C20), the geometry at each metal center could be considered as distorted tetrahedral, in line with stabilization of Cu(I) sites with this geometry. This molecule is asymmetric in the solid state as can be deduced from the  $d_{\text{Cu1}-\text{Cl1}} = 2.61$  Å and  $d_{\text{Cu2}-\text{Cl1}} = 2.49$  Å (Table 2). The Cu1–Cu2 separation of 2.853 Å (with



Table 2. Metal-to-Ligand Distances in the BPMPBCu<sub>2</sub>Cl<sup>+</sup> Complex

	N1	N2	Cl1	C19	C20	N3	N4
Cu1	1.984(3)	1.993(3)	2.6079(10)	2.054(3)	2.053(3)		
Cu2			2.4898(10)	2.053(3)	2.058(3)	1.989(3)	1.988(3)

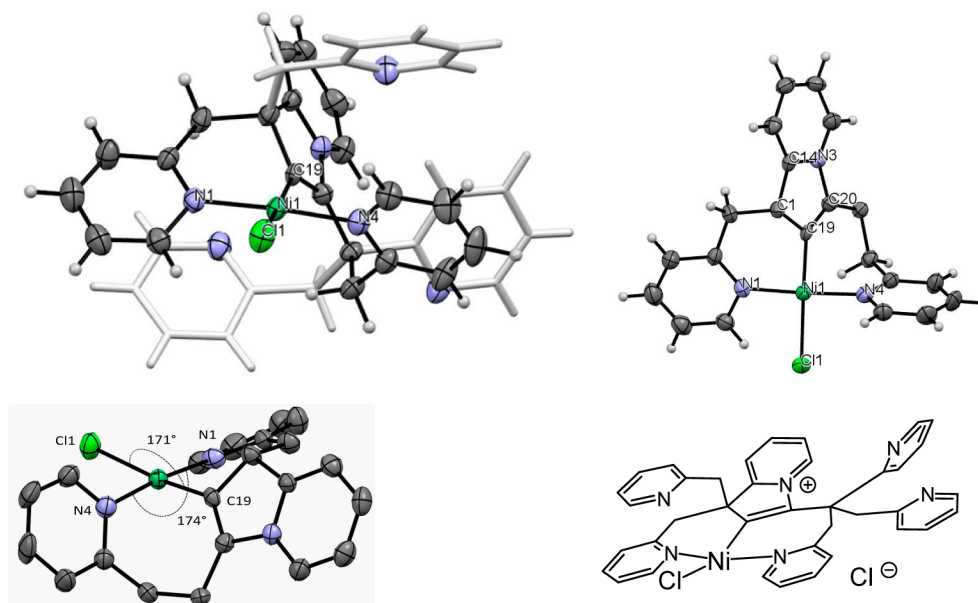


**Figure 7.** ORTEP diagram of the (InBPMPB)NiCl<sup>+</sup> complex with partial labeling: in this drawing, the uncoordinated pyridyl units are in gray. An axial view of the nickel center, and a view of the coordination polyhedron with Cl1NiC19 and N4NiN1 angles. In these two drawings, the uncoordinated pyridyl units have been removed for clarity. Also, finally (lower right), the drawing of the molecule.

Table 3. Selected Distances in the (InBPMPB)NiCl<sup>+</sup> Complex

				Molecule 1				
N1Ni1	N4Ni1	C19Ni1	Cl1Ni1	C19C20	C20N3	N3Cl4	C14C1	C1C19
1.936(4)	1.905(4)	1.859(5)	2.253(1)	1.337(6) <sup>a</sup>	1.461(6) <sup>a</sup>	1.359(6) <sup>a</sup>	1.510(6) <sup>a</sup>	1.500(6) <sup>a</sup>
				Molecule 2				
N7Ni2	N10Ni2	C59Ni2	Cl2Ni2	C60C59	N9C60	C54N9	C41C54	C59C41
1.947(4)	1.903(4)	1.846(5)	2.263(1)	1.346(6) <sup>a</sup>	1.463(6) <sup>a</sup>	1.376(6) <sup>a</sup>	1.505(7) <sup>a</sup>	1.504(6) <sup>a</sup>

<sup>a</sup>Indicates the presence of the indolizinium ring.

$d_{C19-C20} = 1.265(5)$  Å) is close to the distances (ca. 2.80 Å) found in other alkyne-bridged dicopper(I) complexes.<sup>23,24</sup>

Again, the orientation of the pyridyl groups is due to the hydrogen bonds between the nitrogen atom and adjacent methylene groups,  $d_{N5-H6B}$ ,  $d_{N5-H13B}$ ,  $d_{N6-H33B}$ ,  $d_{N6-H26B}$ , being in the 2.4–2.8 Å range.

**Tetragonal Complexes with an Alkenyl Indolizinium Modified Ligand InBPMPB.** The addition of NiCl<sub>2</sub>·6H<sub>2</sub>O to BPMPB in methylene chloride produced a light green color. The addition of diethyl ether to the reaction mixture resulted in the isolation of green precipitate in 66% yield. The complex was characterized with all the spectral studies including ESI-MS, NMR, IR, and electronic absorption spectroscopies. The molecular ion peak of the complex was found at  $m/z = 665.1680$  for (InBPMPBNiCl)<sup>+</sup>. The electronic spectrum for this complex in dichloromethane solution exhibited absorption bands at  $\lambda = 264$  nm ( $\epsilon = 27\,042$  L mol<sup>-1</sup> cm<sup>-1</sup>) and 371 nm ( $\epsilon = 4667$  L mol<sup>-1</sup> cm<sup>-1</sup>). This compound is paramagnetic: its <sup>1</sup>H NMR spectrum in CD<sub>2</sub>Cl<sub>2</sub> clearly showed very broad ( $\delta = 212$  and 184 ppm) to broad ( $\delta = 62, 57, 45, 39, 26, 23, -5$ , and  $-8$  ppm) signals along with a few sharper signals in the diamagnetic region. This latter observation strongly suggests

that part of the ligand only is bound to a paramagnetic center. The trace is displayed in the Supporting Information. Magnetic susceptibility measurements were carried out by the Evans method. The magnetic moment  $\mu_{\text{eff}} = 2.89$   $\mu_B$  was found to be almost identical to that of the expected spin-only moment for a single nickel center ( $\mu_{\text{eff}} = 2.83$   $\mu_B$ ).

Single crystals were obtained from a slow diffusion of diethyl ether into a solution of the complex in dichloromethane in which some drops of methanol were added. The structure was solved, and the ORTEP diagram is displayed in Figure 7. Three main characteristics can be evidenced from this structure: (i) the ligand has been modified, and one pyridine has fused with the alkyne to yield an indolizinium moiety, which is coordinated to the metal through a metal–alkenyl bond; (ii) the BPMPB ligand has become InBPMPB<sup>+</sup>, and a chloride atom (not shown in Figure 7) is present in the structure to balance the positive charge; (iii) this is a mononuclear complex, and one nickel only is linked to the ligand.

Two independent molecules are present in the unit cell, and the metric parameters do not significantly differ. All data are summarized in Table 3. The analysis of the structure reveals relatively short metal-to-ligand distances with  $d_{N1-Ni1} =$

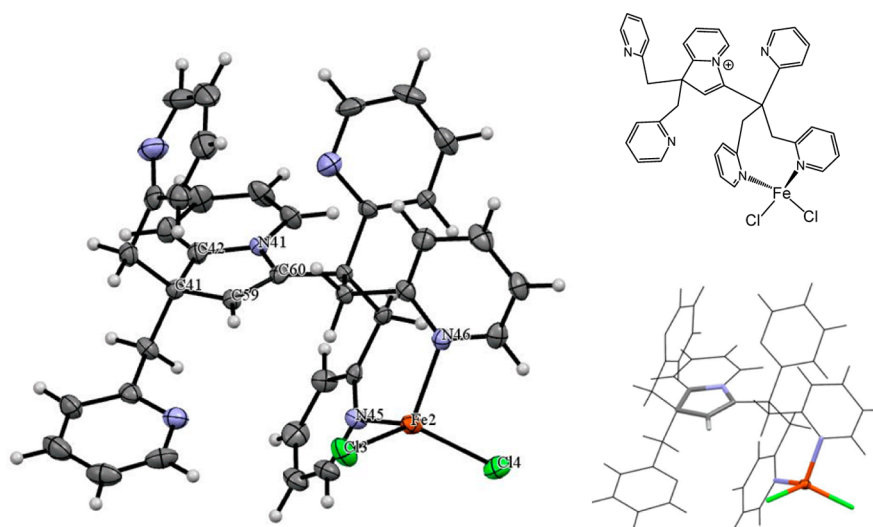


Figure 8. ORTEP diagram of one of the HInBPMPBFeCl<sub>2</sub><sup>+</sup> complexes with partial labeling.

Table 4. Selected Distances in the HInBPMPBFeCl<sub>2</sub><sup>+</sup> Complex

Molecule 1								
N5Fe1	N6Fe1	Cl1Fe1	Cl2Fe1	C19C20	C20N1	N1C2	C2C1	C1C19
2.107(3)	2.116(3)	2.2656(12)	2.2361(13)	1.320(5) <sup>a</sup>	1.467(5) <sup>a</sup>	1.355(5) <sup>a</sup>	1.509(5) <sup>a</sup>	1.506(5) <sup>a</sup>
Molecule 2								
N4SFe2	N46Fe2	Cl3Fe2	Cl4Fe2	C59C60	C60N41	N41C42	C42C41	C41C59
2.116(3)	2.120(3)	2.2581(12)	2.2439(13)	1.329(5) <sup>a</sup>	1.450(5) <sup>a</sup>	1.374(5) <sup>a</sup>	1.492(6) <sup>a</sup>	1.503(5) <sup>a</sup>

<sup>a</sup>Indicates the presence of the indolizinium ring.

1.936(4) Å,  $d_{N4-Ni1} = 1.905(4)$  Å, and  $d_{C19-Ni1} = 1.859(5)$  Å. The indolizinium ring is characterized by  $d_{C19-C20} = 1.337(6)$  Å,  $d_{C20-N3} = 1.461(6)$  Å,  $d_{N3-C14} = 1.359(6)$  Å,  $d_{C14-C1} = 1.510(6)$  Å, and  $d_{C1-C19} = 1.500(6)$  Å.

It is noteworthy that the geometry at the nickel site cannot rigorously be considered as square planar with Cl1NiC19 and N4NiN1 angles of 171° and 174°, respectively. The picture would be that of an almost flat tetrahedron, in line with the paramagnetic character of the complex in solution.

**Tetragonal Complexes with a Free Indolizinium Modified Ligand HInBPMPB. Iron Complex.** Upon addition of FeCl<sub>2</sub> to a solution of BPMPB ligand in CH<sub>2</sub>Cl<sub>2</sub>, a pale green color developed, rapidly followed by a yellow color. The workup under inert atmosphere yielded a caramel brown solid, and the UV-vis spectrum in dichloromethane solution exhibited absorptions at  $\lambda = 261$  ( $\epsilon = 23\,250$  L mol<sup>-1</sup> cm<sup>-1</sup>), 296 ( $\epsilon = 11\,250$  L mol<sup>-1</sup> cm<sup>-1</sup>), and 364 nm ( $\epsilon = 4450$  L mol<sup>-1</sup> cm<sup>-1</sup>). The <sup>1</sup>H NMR of this complex in CDCl<sub>3</sub> exhibited two broad signals at 77 and 46 ppm, with the presence of some sharper resonances in the diamagnetic region. Magnetic susceptibility measurements were carried out by the Evans method on single crystals dissolved in CD<sub>2</sub>Cl<sub>2</sub>. The magnetic moment  $\mu_{\text{eff}} = 8.71$   $\mu_B$  was found to be slightly higher than the expected spin-only moment for a three independent tris-Fe(II) center ( $\mu_{\text{eff}} = 8.48$   $\mu_B$ ).

Single crystals of this compound could be obtained, and the structure was resolved. The unit cell contains two independent molecules. The complex termed [(HInBPMPB)FeCl<sub>2</sub>]<sub>2</sub>[FeCl<sub>4</sub>] was obtained. Here, also, an indolizinium ring, resulting of the fusion of a pyridine with the triple bond, was formed. However, in contrast with the nickel complex, the indolizinium fragment

was uncoordinated. As already mentioned and as the consequence of the formation of an indolizinium, the ligand itself is a charged molecule. In the present structure the charge is equilibrated by a FeCl<sub>4</sub><sup>2-</sup>. The ORTEP diagram of one independent molecule of the complex is displayed in Figure 8.

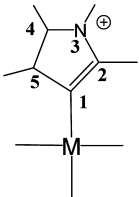
The metal lies in a pseudotetrahedral environment, with two coordinated methylenepyridines and two chloride ions. The metal-to-ligand distances are summarized in Table 4. As already mentioned for the other structures, the conformation of the uncoordinated pyridines is due to intramolecular contacts. In particular, the indolizinium hydrogen interacts with two neighboring N atoms of uncoordinated pyridines with  $d_{NH} = 2.58$  (molecule 1) and  $d_{NH} = 2.55$  Å (molecule 2).

To summarize these results, a variety of different structures could be established from the same ligand, by coordination with different metals. These results will be discussed in the following section.

## DISCUSSION

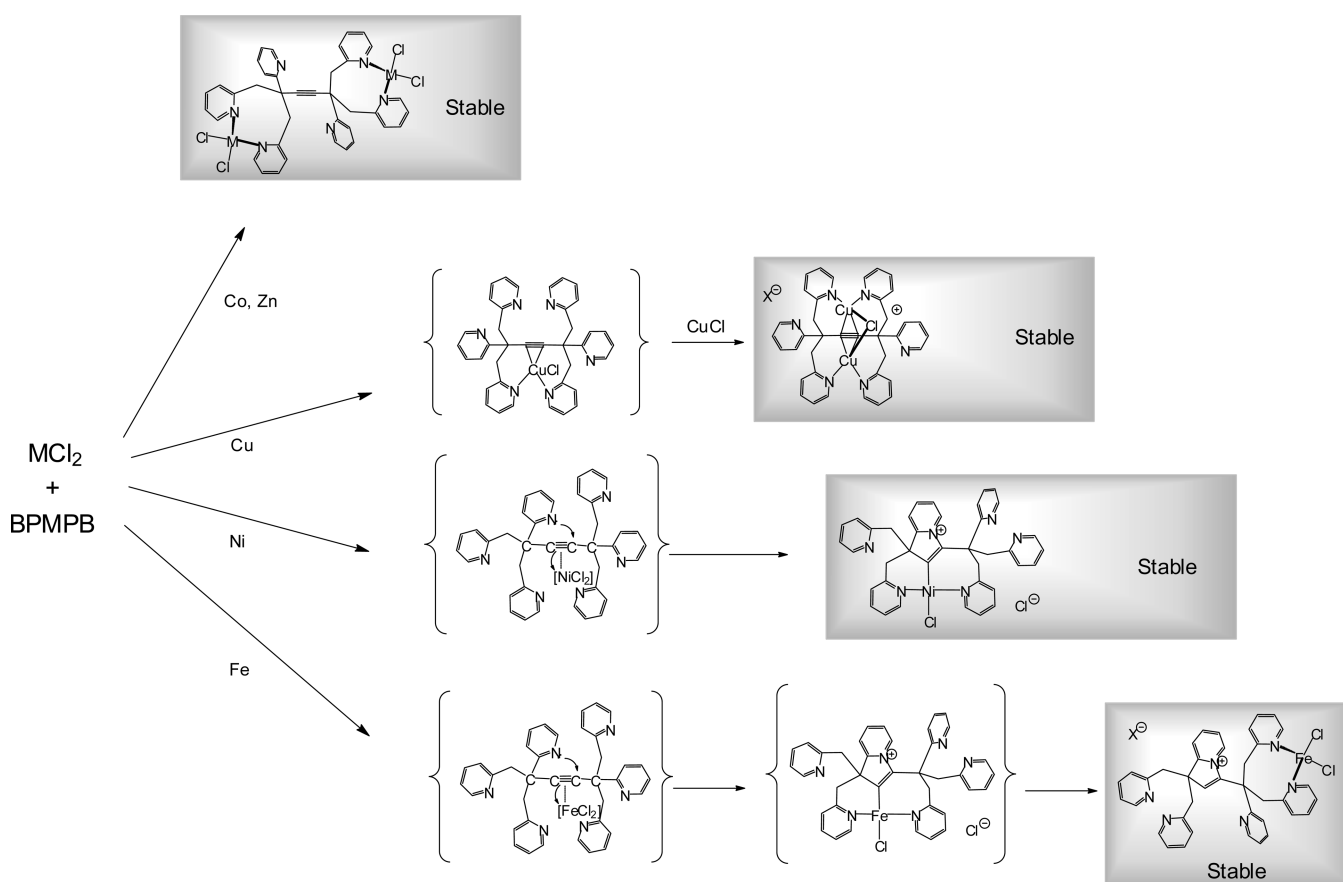
The mechanism of formation of ligand A of Scheme 1 has been proposed, and it involves electrophilic attack of picolyl chloride on stabilized anionic forms of mono- and disubstituted alkyne.<sup>14</sup> In our hands, from A a similar mechanism will ultimately yield BPMPB. By comparison with the 1974 paper, our experiments differ only by the nature of the sodium acetylide, a commercial slurry in our case versus an in situ preparation in the former paper. In the present study, we obtain the BPMPB ligand, plus some dipyridylethene, and ligand A, as shown in the scheme displayed in Supporting Information. Such a difference might arise from differences in the preparation mode of sodium acetylide, which was formerly obtained from sodium amide generated in situ, with different



Table 5. Metric Parameters of the Indolizinium Cycle in the Five Complexes Currently Known<sup>a</sup>


	Ru([9ane]S3Ind 1)	Ru([9ane]S3Ind 2)	Ru([9ane]S3Ind 3)	IndBPMPBNiCl <sub>2</sub> (#1)	HIndBPMPBFeCl <sub>2</sub> <sup>+</sup> (#1)
C1–C2	1.341(3)	1.342(3)	1.338(4)	1.337(6)	1.320(5)
C2–N3	1.441(3)	1.443(3)	1.444(4)	1.461(6)	1.467(5)
N3–C4	1.346(3)	1.350(3)	1.336(4)	1.359(6)	1.355(5)
C4–C5	1.529(3)	1.521(3)	1.516(4)	1.510(6)	1.509(6)
C5–C1	1.550(3)	1.541(3)	1.543(4)	1.500(6)	1.506(5)
	ref 35	ref 35	ref 36	this work	this work

<sup>a</sup>For clarity, the numbering of the cycle is displayed on the drawing above the table.

Scheme 2. General Scheme Summarizing the Different Steps Involved in the Preparation of the Complexes Reported in This Article<sup>a</sup>

<sup>a</sup>The nickel line has been adapted from ref 35. The complexes in brackets are intermediates.

basic properties and possibly containing trace amounts of sodium, responsible for some radical-based reactions, as mentioned in the original paper. Anyway, this point goes beyond the scope of this Article and will not be addressed in the present study.

Regarding coordination chemistry, in none of the complexes reported in the present work does the pyridine coordinate. Only methylenepyridine is bound to the metal. This ligand is well-suited for tetrahedral coordination, at least in methylene chloride which is our solvent.

The coordination of ZnCl<sub>2</sub> and CoCl<sub>2</sub> affords isostructural complexes in the solid state. The coordination is classical and does not lead to particular comments. For the zinc complex, the striking point is the break of symmetry deduced from the <sup>1</sup>H NMR in CD<sub>2</sub>Cl<sub>2</sub>. Our low temperature measurements rule out any possibility of temperature-dependent dynamic process. The only explanation is an asymmetrical conformation of the complex in solution. This is not true in DMSO-*d*<sub>6</sub>, for which a higher symmetry is observed. However, DMSO is a dissociating and potentially coordinating solvent, and the structure might be

different from that seen in the solid state. The cobalt complex is blue and exhibits d–d transitions in UV–vis, in the region where these transitions are generally observed for TPA Co(II) complexes.<sup>25–27</sup> This complex displays a typical paramagnetic <sup>1</sup>H NMR spectrum, indicating the absence of magnetic exchange between the two metal centers within this structure.

Cu(I) was initially chosen to test the ability of the three pyridines of each side of the ligand to provide a tetrahedral environment to a metal–chloride complex. Indeed, this is the case, but we found that the metal coordinated to the alkyne part. This was evidenced in the solid state, but also in solution, as shown from our <sup>13</sup>C NMR measurements which indicate an important downshift of the resonance of the alkyne carbon. Additionally, the <sup>1</sup>H NMR indicated that the symmetry is not broken in solution. Yet, despite being not so common, alkyne-bridged Cu(I) complexes have been known for years,<sup>23,24</sup> and the topic has recently been reviewed.<sup>28</sup> It is noteworthy that the Cu(I) complex is perfectly stable, and does not lead to the formation of indolizinium, as had sometimes been reported.<sup>29</sup>

In the case of NiCl<sub>2</sub>, we were unable to isolate any simple pyridyl-coordinated, or alkyne-coordinated, complexes. Instead, we obtained the InBPMPBNiCl<sup>+</sup> cation, in which the ligand had been converted into the indolizinium cation, which coordinates through the alkenyl fragment. This complex, which can be seen as an indolizine zwitterion Ni-based system, is a mononuclear one, with a Cl<sup>−</sup> anion to balance the charge. At first glance, the geometry of the metal within this compound looks to be square planar. A careful analysis however shows that some distortion toward a tetrahedral geometry occurs, as displayed in Figure 7: this is probably the reason why this complex is paramagnetic, considering that the environment maybe even be more flexible in solution. Any comparison of the UV–vis data with those of the methylenepyridine-containing nickel complex might be daring, since these complexes generally exhibit weak absorption in the visible region<sup>30</sup> and that this is the first Ni–indolizinium complex known today. We might simply postulate that the 371 nm band is due to a charge transfer  $d\pi(\text{NiII}) \rightarrow \pi^*(\text{indolizine})$  MLCT, as is the case for the three related ruthenium complexes (vide infra).

Indolizines, with partially or wholly reduced rings, constitute an important class of compounds due to their biological potential, which includes antimicrobial activity, antioxidant activity, anti-inflammatory activity, anticonvulsant activity, enzyme inhibition activity, and activity as calcium entry blocker.<sup>31,32</sup> The formation of indolizine (not indolizinium) cycles is known in metal-assisted organic chemistry using Cu(I), Cu(II), Au(I), Au(III), Ru(II), Pt(II), Pd(II), Ag(I) and generally involves different pathways.<sup>29,33,34</sup> Formation of indolizinium unit from pyridine–alkyne coupling has very recently been observed in the ruthenium chemistry.<sup>35,36</sup> So far, only three crystal structures were reported on metal–indolizinium complexes, within ruthenium complexes. The present work describes the fourth structure of a metal-bound indolizinium. The metric parameters of the indolizinium ring, including those of the free heterocycle found in the Fe complex, are reported in Table 5 and compared to those of the related ruthenium complexes.

The complex [InBPMPBNiCl]Cl looks like the direct follow-up of [BPMPBCu<sub>2</sub>Cl]Cl as, in the latter, the metal is coordinated to the alkyne in a  $\pi$  fashion. As a consequence, the alkyne is activated toward nucleophilic attack of the neighboring pyridine. Additionally, the geometry and arrangement of the coordination polyhedron prefigure that of the

nickel complex. In the case of a d<sup>10</sup> Cu(I) complex, the alkyne complex is stable, which is not the case for the more Lewis acidic d<sup>8</sup> Ni(II) center. This is summarized in Scheme 2.

During the preparation of the iron complex, we mentioned a transient light green color, prior to a yellow one. The iron complex in the solid state is similar to the nickel one, in which the indolizinium part has been uncoordinated, and the metal center rearranged. The green transient might probably correspond to one of the putative intermediates drawn in Scheme 2, iron line. The origin of the hydrogen atom present on the indolizinium part is uncertain, and could be due to H abstraction from the solvent, or some protonation by small amounts of methanol during the workup.

To conclude, we have reported the coordination chemistry of the new BPMPB ligand, serendipitously obtained as a byproduct of a known reaction. In spite of a modest yield, the facility by which BPMPB is obtained makes it easy to work with. The presence of pyridyl and alkyne coordination sites confers to this ligand some potential in the study of fundamental processes: difference of coordination depending on the nature of the metal, preferred geometry of a given center, or its Lewis acidity leading to ligand modification. Applications of the BPMPB ligand are under study in our group.

## ■ ASSOCIATED CONTENT

### Supporting Information

All NMR and UV–vis spectra. For the reported structures, the crystallographic files in CIF format. The Supporting Information is available free of charge on the ACS Publications website at DOI: 10.1021/acs.inorgchem.5b01096.

## ■ AUTHOR INFORMATION

### Corresponding Author

\*E-mail: dominique.mandon@univ-brest.fr. Phone: ++ 33 (0) 298 016 028. Fax: ++ 33 (0)298 017 001.

### Notes

The authors declare no competing financial interest.

## ■ ACKNOWLEDGMENTS

We thank the Région Bretagne (BioActO2 programm), the CNRS, and the Université de Bretagne Occidentale in Brest. The CEMCA Laboratory in Brest (UMR 6521) is also gratefully acknowledged. We thank all the colleagues from the Service de RMN and Service de Diffraction des Rayons X, of the Faculté des Sciences et Techniques at UBO, Brest. We thank the Agence Nationale de la Recherche (ANR CATHYMETOXY) for financial support. We finally thank Prof. François Petillon (UBO Brest) for helpful discussions and his critical reading of our manuscript.

## ■ REFERENCES

- (1) Blackman, A. G. *Polyhedron* **2005**, *24*, 1–39.
- (2) Blackman, A. G. *Eur. J. Inorg. Chem.* **2008**, *2008*, 2633–2647.
- (3) Talsi, E. P.; Bryliakov, K. P. *Coord. Chem. Rev.* **2012**, *256*, 1418–1434.
- (4) Mannich, M. P.; Mohs, P. *Ber. Dtsch. Chem. Ges. B* **1930**, *63B*, 608–612.
- (5) Comba, P.; Lee, Y.-M.; Nam, W.; Waleska, A. *Chem. Commun.* **2014**, *50*, 412–414.
- (6) Comba, P.; Kersch, M.; Schiek, W. *Prog. Inorg. Chem.* **2007**, *55*, 613–704.
- (7) Comba, P. *Mol. Catal.* **2014**, 123–145.

- (8) Klopstra, M.; Roelfes, G.; Hage, R.; Kellogg, R. M.; Feringa, B. L. *Eur. J. Inorg. Chem.* **2004**, 2004, 846–856.
- (9) McQuilken, A. C.; Jiang, Y. B.; Siegler, M. A.; Goldberg, D. P. J. *Am. Chem. Soc.* **2012**, 134, 8758–8761.
- (10) Sahu, S.; Widger, L. R.; Quesne, M. G.; de Visser, S. P.; Matsumura, H.; Moënné-Loccoz, P.; Siegler, M. A.; Goldberg, D. P. J. *Am. Chem. Soc.* **2013**, 135, 10590–10593.
- (11) Widger, Leland R.; Jiang, Y.; McQuilken, Alison C.; Yang, Tzuhsung; Siegler, Maxime A.; Matsumura, Hirotoshi; Moënné-Loccoz, Pierre; Kumar, Devesh; de Visser, Sam P.; Goldberg, David P. *Dalton Trans.* **2014**, 43, 7522–7532.
- (12) Kodera, M.; Itoh, M.; Kano, K.; Funabiki, T. *Bull. Chem. Soc. Jpn.* **2006**, 79, 252–261.
- (13) Kodera, M.; Kano, K. *Bull. Chem. Soc. Jpn.* **2007**, 80, 662–676.
- (14) Zune, A. E.; Hollstein, U.; Litchman, W. M. *J. Org. Chem.* **1974**, 39, 2461–2463.
- (15) Litchman, W. M.; Zune, A. E.; Hollstein, U. *J. Magn. Reson.* **1975**, 17, 241–243.
- (16) We work at each step with different metals. The purpose of this study is to present snapshots on structures possibly involved in the conversion.
- (17) Evans, D. F. *J. Chem. Soc.* **1959**, 2003–2005.
- (18) Evans, D. F.; Jakubovic, D. A. *J. Chem. Soc., Dalton Trans.* **1988**, 2927–2933.
- (19) Bain, G. A.; Berry, J. F. *J. Chem. Educ.* **2008**, 85, 532–536.
- (20) Altomare, A.; Cascarano, G.; Giacovazzo, C.; Guagliardi, A.; Burla, M. C.; Polidori, G.; Camalli, M. *J. Appl. Crystallogr.* **1994**, 27, 435–436.
- (21) Vansant, J.; Smets, G.; Declercq, J. P.; Germain, G.; Van Meerssche, M. *J. Org. Chem.* **1980**, 45, 1557–1565.
- (22) A computer-assisted search revealed the occurrence of structurally characterized (1,2-bis(2-pyridyl)ethylene) in eight references.
- (23) Villacorta, G. M.; Gibson, D.; Williams, I. D.; Whang, E.; Lippard, S. J. *Organometallics* **1987**, 6, 2426–2431.
- (24) Reger, D. L.; Huff, M. F.; Wolfe, T. A.; Adams, R. D. *Organometallics* **1989**, 8, 848–850.
- (25) Massoud, S. S.; Perkins, R. S.; Louka, F. R.; Xu, W.; Le Roux, A.; Dutercq, Q.; Fischer, R. C.; Mautner, F. A.; Handa, M.; Hiraoka, Y.; Kreft, G. L.; Bortolotto, T.; Terenzi, H. *Dalton Trans.* **2014**, 43, 10086–10103.
- (26) Wang, H.; Lu, Y.; Mijangos, E.; Thapper, A. *Chin. J. Chem.* **2014**, 32, 467–473.
- (27) Massoud, S. S.; Broussard, K. T.; Mautner, F. A.; Vicente, R.; Saha, M. K.; Bernal, I. *Inorg. Chim. Acta* **2008**, 361, 123–131.
- (28) Lang, H.; Jakob, A.; Milde, B. *Organometallics* **2012**, 31, 7661–7693.
- (29) Seregin, I. V.; Schammel, A. W.; Gevorgyan, V. *Tetrahedron* **2008**, 64, 6876–6883.
- (30) He, Z.; Craig, D. C.; Colbran, S. B. *J. Chem. Soc., Dalton Trans.* **2002**, 4224–4235.
- (31) Singh, G. S.; Mmatli, E. E. *Eur. J. Med. Chem.* **2011**, 46, 5237–5257.
- (32) Sharma, V.; Kumar, V. *Med. Chem. Res.* **2014**, 23, 3593–3606.
- (33) Zhang, C.; Zhang, H.; Zhang, L.; Wen, T. B.; He, X.; Xia, H. *Organometallics* **2013**, 32, 3738–3743.
- (34) Sun, J.; Wang, F.; Hu, H.; Wang, X.; Wu, H.; Liu, H. *J. Org. Chem.* **2014**, 79, 3992–3998.
- (35) Chung, L. H.; Wong, C. Y. *Organometallics* **2013**, 32, 3583–3586.
- (36) Chung, L. H.; Yeung, C. F.; Ma, D. L.; Leung, C. H.; Wong, C. Y. *Organometallics* **2014**, 33, 3443–3452.